The interplay between total mercury, methylmercury and dissolved organic matter in fluvial systems: A latitudinal study across Europe

Andrea G. Bravo[1,*,+], Dolly N. Kothawala[2,+], Katrin Attermeyer[2], Emmanuel Tessier[3], Pascal Bodmer[4,5], José L. J. Ledesma[6], Joachim Audet[6], Joan Pere Casas-Ruiz[7], Núria Catalán[7], Sophie Cauvy-Fraunié[8], Miriam Colls[7], Anne Deininger[9], Vesela V. Evtimova[10], Jérémy A. Fonvielle[11], Thomas Fuß[12,13], Peter Gilbert[14], Sonia Herrero Ortega[11], Liu Liu[5], Clara Mendoza-Lera[8], Juliana Monteiro[15], Jordi-René Mor[7,16], Magdalena Nagler[17], Georg H. Niedrist[18], Anna C. Nydahl[2], Ada Pastor[7], Josephine Pegg[19,20], Catherine Gutmann Roberts[19], Francesca Pilotto[9], Ana Paula Portela[15], Clara Romero González-Quijano[12], Ferran Romero[7], Martin Rulík[21], David Amouroux[3,*]

[1] Department of Environmental Chemistry, Institute of Environmental Assessment and Water Research (IDAEA), Spanish National Research Council (CSIC), Barcelona, Spain
[2] Limnology/Department of Ecology and Genetics, Uppsala University, Uppsala, Sweden
[3] CNRS/ UNIV PAU & PAYS ADOUR, Institut des Sciences Analytiques et de Physico-Chimie pour l'Environnement et les Materiaux, UMR5254, MIRA, Pau, France
[4] Institute for Environmental Sciences, University of Koblenz-Landau, Landau, Germany
[5] Chemical Analytics and Biogeochemistry, Leibniz-Institute of Freshwater Ecology and Inland Fisheries, Berlin, Germany
[6] Department of Aquatic Sciences and Assessment, Swedish University of Agricultural Sciences, Uppsala, Sweden
[7] Catalan Institute for Water Research (ICRA), Girona, Spain
[8] IRSTEA, UR RIVERLY, 69616 Villeurbanne Cedex, France
[9] Department of Ecology and Environmental Science, Umeå University, Umeå, Sweden
[10] Department of Aquatic Ecosystems, Institute of Biodiversity and Ecosystem Research, Bulgarian Academy of Sciences, Sofia, Bulgaria
[11] Experimental Limnology, Leibniz-Institute of Freshwater Ecology and Inland Fisheries (IGB), Stechlin, Germany
[12] Ecohydrology, Leibniz-Institute of Freshwater Ecology and Inland Fisheries (IGB), Berlin, Germany
[13] WasserCluster Biological Station Lunz, Lunz am See, Austria
[14] The Environmental Research Institute, University of Highlands and Islands, Thurso, Scotland, UK,
[15] Research Centre in Biodiversity and Genetic Resources (CIBIO), University of Porto, Porto, Portugal
[16] Department of Evolutionary Biology, Ecology and Environmental Sciences, Faculty of Biology, University of Barcelona (UB), Barcelona, Spain
[17] Microbial Resource Management, Institute of Microbiology, University of Innsbruck, Innsbruck, Austria
[18] River and Conservation Research, Institute of Ecology, University of Innsbruck, Innsbruck, Austria
[19] Department of Life and Environmental Sciences, Bournemouth University, UK
[20] University Centre Sparsholt, Winchester, UK
[21] Department of Ecology and Environmental Sciences, Palacky University in Olomouc, Olomouc, Czech Republic

[+] These authors contributed equally to this work.
Corresponding authors: Andrea G Bravo (jandriugarcia@gmail.com) & David Amouroux (david.amouroux@univ-pau.fr)

Keywords: Mercury, methylmercury, streams, rivers, freshwaters, organic matter, EuroRun, fluorescence

Abstract

Large-scale studies are needed to identify the drivers of total mercury (THg) and monomethyl-mercury (MeHg) concentrations in aquatic ecosystems. Studies attempting to link dissolved organic matter (DOM) to levels of THg or MeHg are few and geographically constrained. Additionally, stream and river systems have been understudied as compared to lakes. Hence, the aim of the study was to examine the influence of DOM concentration and composition, morphological descriptors, land uses and water chemistry on THg and MeHg concentrations and the percentage of THg as MeHg (%MeHg) in 29 streams across Europe spanning from 41°N to 64 °N. THg concentrations (0.06 – 2.78 ng L^{-1}) were highest in streams characterized by DOM with a high terrestrial soil signature and low nutrient content. MeHg concentrations (78 – 160 pg L^{-1}) varied non-systematically across systems. Relationships between DOM bulk characteristics and THg and MeHg suggest that while soil derived DOM inputs control THg concentrations, autochthonous DOM (aquatically produced) and the availability of electron acceptors for Hg methylating microorganisms (e.g. sulfate) drive %MeHg and potentially MeHg concentration. Overall, these results highlight the large spatial variability in THg and MeHg concentrations at European scale, and underscore the importance of DOM composition on Hg cycling in fluvial systems.

1. INTRODUCTION

Mercury (Hg) is a hazardous substance with the potential to produce significant adverse neurological and other health effects in severely exposed humans, with particular concerns on unborn children and infants (Mason et al., 2012). Anthropogenic emissions and long-range transport of atmospheric-Hg have led to Hg concentrations above background levels in surface reservoirs (atmosphere, oceans or terrestrial) on a global scale (Amos et al., 2013). Aquatic food webs are particularly vulnerable to increases in Hg, since its methylated form (monomethyl-mercury, MeHg) accumulates in organisms and biomagnifies in aquatic food webs (Morel et al., 1998), even at low concentrations. As a consequence, millions of people are readily exposed to harmful concentrations of MeHg via fish consumption (Mason et al., 2012).

In order to prevent human exposure to Hg, a global legally binding agreement, the Minamata Convention, was signed by 128 countries and entered into force in September 2017. Prior to the Minamata Convention, the European Water Framework Directive (WFD, 2008) classified Hg as one of 30 priority hazardous substances and set the maximum allowable concentrations of environmental quality standards to 70 ng L^{-1}. However, in aquatic systems, without any point anthropogenic or geological sources, total-Hg (THg) concentration typically ranges from less than 0.05 to 12 ng L^{-1} (Dennis et al., 2005; Driscoll et al., 2007; Wiener et al., 2003). Because the maximum allowable concentrations of environmental quality standards were much higher than naturally relevant concentration levels of THg, national monitoring programs did not have the incentive to detect THg at ambient concentrations. There is even less information about MeHg background levels, which generally are between one and two orders of magnitude lower as compared to THg levels (Driscoll et al., 2007). In this context, streams and rivers are of special concern because very few studies have reported THg and MeHg concentrations at a wide geographical scale (Balogh et al., 2002; Brigham et al., 2009; Eklöf et al., 2015; Lescord et al., 2018; Marvin-DiPasquale et al., 2009; Tsui et al., 2009). While rivers and streams have, however, been hypothesized to be important contributors to the global biogeochemical Hg budget (Amos et al., 2014; Kocman et al., 2017; Schartup et al., 2015a; Sunderland and Mason, 2007), quantitative information on Hg levels is largely lacking, especially in the temperate zone. Filling this gap in knowledge is an important prerequisite in the ongoing quest to reduce uncertainties associated with the global biogeochemical cycling of Hg and for the development of remediation and risk management strategies within the context of the Minamata Convention.

Freshwaters receive Hg from a variety of sources including atmospheric deposition (Fitzgerald et al., 1998), release from industrial discharge (Bravo et al., 2015, 2014), and lateral export from terrestrial sources (e.g. soils and wetlands) (Brigham et al., 2009; Eklöf et al., 2012). Diffuse inputs from land management activities and remobilization of Hg previously accumulated in terrestrial ecosystems can be an important source comparable in

magnitude to direct Hg anthropogenic inputs (e.g. industrial releases or mining activities) to surface waters (Kocman et al., 2017). Long-term accumulation of Hg in terrestrial systems has been explained by the strong binding between atmospherically deposited Hg and sulfur sites within organic matter (OM) (Skyllberg et al., 2006; Xia et al., 1999). In boreal ecosystems, characterized by OM-rich soils, the strong correlation between THg and dissolved organic carbon (DOC) found in several studies (Brigham et al., 2009; Driscoll et al., 1995; Eklöf et al., 2012; Tsui et al., 2009) denotes that the mobilization of OM is an important vector for Hg transport from catchment soils to surface waters (Eklöf et al., 2012; Grigal, 2002). Besides stream water DOC, the proportion of wetland area within the catchment and the discharge have been used to predict THg concentrations in surface waters (Brigham et al., 2009; Eklöf et al., 2015; Tsui et al., 2009). In contrast, the relationship between DOC and MeHg remains poorly understood (Brigham et al., 2009; Tsui et al., 2009). The variation of MeHg concentrations in aquatic ecosystems is indeed more complex, as MeHg is potentially derived from numerous sources, not only terrestrial sources. In boreal streams, the wetland proportion of the catchment has also been linked to MeHg freshwater concentrations (Brigham et al., 2009). Wetlands, characterized by oxygen-depletion and low to intermediate nutrient levels, are known to be important sites for MeHg production and a relevant source of MeHg to inland waters (Schaefer et al., 2014; Tjerngren et al., 2012). Besides the contribution of MeHg produced in wetlands to stream waters, in-stream MeHg formation might also be an additional key source of MeHg (Balogh et al., 2002; Eklöf et al., 2015; Tsui et al., 2009), especially in catchments lacking extensive wetland coverage. The methylation of inorganic divalent Hg (IHg) to MeHg is primarily mediated by anaerobic micro-organisms (Gilmour et al., 2013) and is controlled by temperature, availability of electron acceptors (e.g. SO_4^{2-} and Fe^{3+}) (Bravo et al., 2015) and the molecular composition of OM, which influences IHg-speciation (Graham et al., 2013; Jonsson et al., 2014), IHg-availability (Chiasson-Gould et al., 2014; Mazrui et al., 2016; Schaefer and Morel, 2009; Schartup et al., 2015b) and microbial activity (Bravo et al., 2017). Specifically, IHg methylation processes are enhanced by the presence of algal OM (Bravo et al., 2017; Schartup et al., 2013) and fresh humic OM

leached from organic rich soils (Herrero Ortega et al., 2018). Indeed, elevated MeHg concentrations have been linked to periods of high algal production (Gascon Diez et al., 2016; Soerensen et al., 2017) and leaf fall (Balogh et al., 2002). However most studies investigating the role of OM as a transport vector for Hg and/or a key factor controlling MeHg formation have been carried out in the boreal biome. Consequently, there is still a high amount of uncertainty in identifying factors governing THg and MeHg levels in stream waters, particularly at a broader geographical scale.

The molecular composition of dissolved organic matter (DOM) is variable and can be an important factor in predicting THg and potentially, MeHg (Bravo et al., 2017; Herrero Ortega et al., 2018; Lescord et al., 2018; Noh et al., 2017; Schartup et al., 2015b, 2013). A common fingerprinting approach used to characterize the bulk DOM composition in inland waters is fluorescence spectroscopy (Fellman et al., 2010). The increasingly widespread use of fluorescence can be attributed to its wide accessibility, ease of use, and low costs. Three commonly used indexes (fluorescence index (McKnight et al., 2001), freshness index (Parlanti et al., 2000) and humification index (Zsolnay et al., 1999)) are particularly useful for distinguishing between DOM derived from different sources (McKnight et al., 2001), and degrees of freshness and humification (Zsolnay et al., 1999). Likewise, commonly known re-occurring peaks distributed across the fluorescence excitation-emission matrix (EEM) can provide insights into sample specific DOM characteristics. Fluorescence has indeed demonstrated the potential to reveal key DOM molecular characteristics associated with THg and MeHg concentrations (Herrero Ortega et al., 2018; Lescord et al., 2018; Noh et al., 2017; Schartup et al., 2015b).

The aim of this study was to identify the relationships between THg and MeHg concentrations and DOM composition (sources and quality) across a diversity of European streams. Unraveling the factors determining THg and MeHg background levels in the aquatic environment at a broad geographical scale is crucial for a better understanding of Hg cycling. For this purpose, we measured THg and MeHg concentrations, DOM concentration and

composition, anions and cations in filtered and unfiltered stream water at 29 sites with contrasting catchment characteristic across a wide latitudinal gradient across Europe.

2. MATERIAL AND METHODS

2.1 Organizational Framework

Water sampling for THg and MeHg concentration measurements was organized within the framework of the project called EuroRun: *Assessing CO_2 fluxes from European running waters* (available from https://freshproject-eurorun.jimdo.com/). EuroRun represents the first Collaborative European Freshwater Science Project for Young Researchers aiming to create synergistic interactions among young and early career scientists across Europe. Within the context of the collaborative EuroRun project, the EuroRun_Mercury initiative included 12 teams distributed in 8 countries, which sampled 29 stream sites (Fig. 1). With 56% of participants being female, EuroRun_Mercury was gender balanced. The teams represented different regions across Europe. For a specific region, each team selected several sites with contrasting dominant land uses (i.e. forest or agriculture) and a wide range of hydrological and watershed characteristics (Table S1).

2.2 Sampling

The sampling procedure was explained and demonstrated to one lead representative from each team, who participated in a workshop performed in Sweden in September 2016. All the material needed to collect water samples along with a detailed written protocol was provided to participants during the workshop (see SI). The sampling took place during 3rd – 14th October 2016 and teams from Austria (AUT), Bulgaria (BGR), the Czech Republic (CZE), Germany (DEU), Spain (ESP), France (FRA), Great Britain (GBR), Portugal (PRT) and Sweden (SWE) collected water samples for this study (Fig. 1). The 29 sampled sites were located across a wide latitudinal gradient (from 41°N to 64 °N) and altitude range (from 1 to 1560 m above sea level), and spanned a wide range of hydrological (discharge from 0.1 to 56 m^3 s^{-1}) and catchment characteristics (Table S1). Each team provided hydrological

(discharge, stream wetted width and stream order) and catchment characteristics data (land use in % and catchment area).

A total of 4 water samples were collected at each site. Amber borosilicate bottles (VWR, 250 mL) were used to store water and analyze THg and MeHg species in filtered and unfiltered fractions. A previous study determined the cleaning procedures suitable for THg and MeHg analyses with these bottles (Cavalheiro et al., 2016). In the field, borosilicate bottles were rinsed three times with filtered (0.45 µm, Sterivex-HV) or unfiltered water. For dissolved ($_D$) THg_D and $MeHg_D$ analyses about 250 mL of water were collected directly into the amber borosilicate bottle, filtered (0.45 µm, Sterivex-HV) and acidified (1% v/v final concentration; HCl Ultrex II, J. T. Baker) on site. A subsample of filtered water was placed into 40 mL pre-muffled EPA borosilicate glass vials (VWR) with PTFE caps for analysis of DOC concentration, DOM optical properties and concentration of anions and cations. Unfiltered water samples were collected for determination of the total fraction ($_T$) of THg_T, $MeHg_T$ (acidified) and total organic carbon (TOC) concentration. Samples were kept at 4°C and shipped to the laboratory by courier within 48 h. A subsample (10 mL) of unfiltered water was filtered in the laboratory, and stored frozen for later determination of anions and cations. Because four of the vials broke during transport, these samples could not be determined (marked as not determined in Table 1 and S2).

Results for unfiltered water samples correspond to the total fraction (THg_T, $MeHg_T$ and TOC), whereas the results for filtered water samples represent the dissolved fraction (THg_D, $MeHg_D$, DOC, DOM optical properties, anions and cations).

2.3 Chemical Analyses

2.3.1 Analysis of Inorganic-Hg and Methylmercury

Inorganic-Hg (IHg) and MeHg (monomethylmercury) concentrations (Table 1) were measured using species-specific isotope dilution and capillary gas chromatography (Trace GC Ultra, Thermo Fisher, Waltham, MA, USA equipped with a TriPlus RSH auto-sampler) hyphenated to inductively coupled plasma mass spectrometer (Thermo X Series 2)

(Cavalheiro et al., 2016; Rodriguez Martín-Doimeadios et al., 2003). The detection limits of this method are 0.02 ng L^{-1} for IHg and 0.005 ng L^{-1} for MeHg. The measurement error (calculated by analyzing each sample three times) was less than 15% and 10% for IHg and MeHg concentrations, respectively. Based on previous studies (Bravo et al., 2014; Monperrus et al., 2004; Rodriguez Martín-Doimeadios et al., 2003), THg was calculated as the sum of IHg and MeHg.

2.3.2 TOC, DOC and DOM optical properties

TOC and DOC concentrations were determined on unfiltered and filtered samples, respectively. Prior to analysis, samples were acidified to a pH of 2 with 0.1 M HCl, and analyzed using a Shimadzu TOC-V_{CPH} total carbon analyzer. Optical properties were determined on filtered water using an Aqualog spectrofluorometer (Horiba), which measures absorbance and fluorescence simultaneously. The fluorescence spectrophotometer has a routine protocol before running samples that involves i) instrument validation (ensuring the signal : noise ratio <20,000 counts ii) ensuring the excitation lamp is calibrated to a given wavelength (maximum intensity at 467 nm), iii) the emission energy is calibrated using pure water at an emission of 397 nm and an excitation of 350 nm. Fluorescence spectra were collected across excitation wavelengths (Ex_λ) 250 to 445 nm at 5 nm increments and across emission wavelengths (Em_λ) ranging from 300–600 nm. Bandpass and resolution were 5 nm. All spectra were measured in a 1 cm quartz cuvette and automatically blank-subtracted, corrected for instrument biases and inner filter effects using the FluorEssence™ software (Horiba). Samples were measured for fluorescence at a 2 second integration time, with the exception of five more optical dense samples from Great Britain and Sweden, which were measured at 0.5 seconds. All intensities were normalized to 1 second integration time post-analysis and the excitation-emission matrixes (EEM) were expressed in fluorescence units (FU).

Peak picking was used to define the relative intensity of four common peaks across the EEM including the Peak A (λ_{ex}: 260 nm, λ_{em}: 400–460 nm), Peak C (λ_{ex}: 320–360 nm, λ_{em}: 420–460 nm), and Peak M (λ_{ex}: 290–310 nm, λ_{em}: 370–410 nm) associated with soil

terrestrial DOM, as well as a protein-like peak T (λ_{ex}: 275 nm, λ_{em}: 340–350 nm) that is considered to be of algal/bacterial origin (i.e. autochthonous to the aquatic environment) (Fellman et al., 2010; Huguet et al., 2009). The summed area of total fluorescence (TF) under the EEMs was used to normalize each of the four peaks, which were expressed as a percent of TF (i.e. %Peak A = Peak A/ TF x 100%). We also calculated three common fluorescence indexes: i) the fluorescence index (FI, calculated as the ratio between emission at wavelengths of 470 and 520 nm, at an excitation of 370 nm), an indicator of source being more microbial (≈1.8) or terrestrial (≈1.2) (Cory et al., 2007; McKnight et al., 2001), ii) the freshness index (calculated as the ratio of emission at 380 nm, divided by the emission maxima between 420 and 435 nm, at an excitation of 310 nm) which reflects the age of OM, with higher values representing more recently produced OM (Parlanti et al., 2000) and iii) the humification index (HIX, ratio of peak areas across an emission spectra [435–480 nm / 300–345 nm]), indicating the degree of humification (Zsolnay et al., 1999). The absorbance at 254 nm (A_{254}) was used to calculate carbon specific absorbance ($SUVA_{254}$), a commonly used metric of the degree of aromaticity, as A_{254}/DOC concentration normalized to a 1 m path length (L mg C^{-1} m^{-1}) (Weishaar et al., 2003).

2.3.3 Anions and Cations

Inorganic analyses were conducted on a Metrohm IC system (883 Basic IC Plus and 919 Autosampler Plus). Anions (F^-, Cl^-, NO_3^- and SO_4^{2-}) were separated on a Metrosep A Supp 5 analytical column (150 x 4.0 mm) fitted with a Metrosep A Supp 4/5 guard column at 0.7 mL min^{-1} using a carbonate eluent (3.2 mM Na_2CO_3 + 1.0 mM $NaHCO_3$). A Metrosep C4 column (250 x 2.0 mm) with a Metrosep C4 guard column was used for separation of the cations (Na^+, NH_4^+, K^+, Ca^{2+}, Mg^{2+}) with an eluent of 1.7 mM nitric acid and 0.7 mM dipicolinic acid at a flow rate of 0.2 mL min^{-1}.

2.4 Statistical Analyses

Kolmogorov–Smirnov test and quantile–quantile plots were used to evaluate the normality of the data. The distribution of THg concentrations were slightly skewed due to the high concentrations measured at sites in Great Britain. The center and dispersion of THg

concentrations were summarized by the median and the inter-quartile range (IQR). DOM optical parameters, MeHg and %MeHg met normality after being log-transformed. Parametric tests were used to analyze linear correlations (Pearson) between DOM optical parameters, THg and MeHg concentrations, and %MeHg and to compare Hg concentrations in the total and dissolved fractions (t-test). All statistical tests were carried out in R 3.2.4 (http://www.R-project.org/) (R Core Team, 2016).

Principle component analysis (PCA) was used as an initial diagnostic tool to examine key relationships and identify strongly correlated variables including optical measurements (i.e. %Peak A, %Peak C, %Peak M and %Peak T, $SUVA_{254}$, fluorescence index, freshness index, humification index), TOC, sulfate, nitrate and calcium concentrations, land use and stream order. This complete information was available for 21 of the 29 studied sites. Accordingly, the samples with incomplete information (DEU1_1, DEU1_2, GBR2_2, FRA1_2, PRT1_1, CZE1_1, GBR2_1 and ESP2_3) were excluded from the PCA analysis. All data were log-transformed, scaled and centered prior to PCA analysis. PCA analysis were carried out using the *prcomp* function of the package *stats* in R 3.2.4 (R Core Team, 2016).

Partial least squares (PLS) regression models were subsequently applied to predict THg concentration (Y response variable) from DOM optical properties, water chemistry and catchment characteristics (X predictor variables, Table S5 and Table S6). A second PLS, excluding the sites with high THg concentrations (Great Britain, GBR1_1, GBR1_2), was also tested (Supplementary information, Table S7). The PLS model performance was examined based on the cumulative goodness of fit (R^2Y, explained variation), and the cumulative goodness of prediction (or Q^2, predicted variation). The variable influence on projections (VIP scores) provided a means of assigning the importance of X variables on the overall PLS model. X-predictor variables with an influence score ≥1 were considered highly influential, between 0.8 and 1.0 moderately influential, and <0.8 less influential predictors (Eriksson et al., 1999). The PLS models were performed using the *plsr* function of the *pls* package in R (Mevik and Wehrens, 2007). Graphics were built in R 3.2.4 (R Core Team, 2016) and modified to fit the journal requirements with Inkscape 0.92 (https://inkscape.org/es/).

305 THg and MeHg loads of both total and dissolved fractions (Table S3) were calculated
306 with the stream discharge value provided by the participants (Table S1) and the
307 concentrations measured in this study (Table 1).

308 **3. RESULTS**

309 **3.1 Mercury Levels (THg, IHg, MeHg and %MeHg)**

310 THg concentrations were consistently low among sites (Table 1). Median values for
311 total (THg_T) and dissolved fractions (THg_D) were 0.46 ng L^{-1} (interquartile range, IQR: 0.28 –
312 0.8) and 0.24 ng L^{-1} (IQR: 0.28 – 0.49), respectively. Streams in Great Britain (GBR) and
313 Austria (AUT) had the highest THg_T and THg_D concentrations (Fig. 2a, Table 1). THg_T
314 concentrations were generally higher than THg_D ($p = 0.004$), although both were significantly
315 correlated (R^2=0.62, $p = 0.04$; Table S3). IHg_T was also slightly higher than IHg_D (Fig. 2b).
316 $MeHg_T$ concentrations ranged between 7.8 and 159 pg L^{-1} and were similar ($p = 0.07$) to
317 $MeHg_D$ (6.6 – 134 pg L^{-1}; Fig. 2c). The highest MeHg concentrations, for total and dissolved
318 fractions, were found at sites from Sweden (SWE2_1), Great Britain (GBR1_1) and Spain
319 (ESP1_3). The %MeHg was very similar in both the total ($\%MeHg_T$) and dissolved ($\%MeHg_D$)
320 fractions (Fig. 2d) but varied among sites, ranging from 1 to 43%. The highest $\%MeHg_T$ was
321 found at a Spanish site (ESP1_3). The median of THg_T and $MeHg_T$ loads were 3.9 kg $year^{-1}$
322 (IQR: 0.6 – 6.8) and 0.3 kg $year^{-1}$ (IQR: 0.1 – 0.5), respectively.

323 Significant correlations were found between the total and dissolved fraction of THg,
324 IHg and MeHg (Table S3). As total and dissolved fractions were correlated, we used the total
325 fraction (THg_T, $MeHg_T$, $\%MeHg_T$) for all the following statistical analyses (PCA and PLS).

326 **3.2 Water Chemistry**

327 DOC and TOC concentrations ranged between 0.9 and 18.5 mg L^{-1} and 0.9 and 22.2
328 mg L^{-1}, respectively. DOC and TOC were significantly correlated ($R^2 = 0.99$, $p < 0.01$). The
329 highest concentrations were found in Great Britain (GBR1_1, GBR1_2) and Sweden
330 (SWE1_1) and the lowest in Spain (ESP1_2, ESP2_1) and Austria (AUT2_1, AUT2_2,
331 AUT2_3; Table S2). The concentrations of sulfate, a well-known electron acceptor for Hg
332 methylating microorganisms, varied largely and ranged from 1.3 (AUT1_1) to 731 (ESP2_3)

mg L^{-1}. About 50% of the studied sites presented sulfate concentrations lower than 12.6 mg L^{-1} (IQR: 6.8 – 66 mg L^{-1}). Spanish sites presented the highest sulfate concentrations (Table S2). Nitrate concentration varied between 0.04 (GBR1_1) and 23 (ESP2_2) mg L^{-1}. The median value for nitrate concentration was 1.9 mg L^{-1} (IQR: 0.7 – 2.7).

3.3 DOM Optical Characteristics

Very distinct fluorescence signatures were observed between study sites, with four illustrative EEMs representing contrasting signatures displayed in Figure 3. Sites from Great Britain showed a strong optical signature representing terrestrially derived DOM, as indicated by the high intensity of Peaks A and C, while in contrast, sites from Spain (ESP) and the Czech Republic (CZE), with high Peak T intensities, represented DOM optical signatures of waters typically enriched in autochthonous DOM (Fig. 3, Table S2). The wide range of bulk DOM optical characteristics captured in this dataset can be attributed to the broad geographical scale of this study.

Analyzed water samples also captured a wide range of DOM characteristics based on each of the measured optical indexes. The $SUVA_{254}$, which is associated with the presence of aromatic (Weishaar et al., 2003) and high molecular mass compounds (Chowdhury, 2013) typically spans from <1 to a maximum of 6 L mg C^{-1} m^{-1} (Weishaar et al., 2003), and was found to range from 2.4 (CZE1_2) to 5.2 (GBR1_1, GBR1_2) L mg C^{-1} m^{-1}. HIX values spanned from 2.2 to 25 (Table S2). The highest HIX values were measured in Austria (AUT1_2) and Great Britain (GBR1_1, GBR1_2). Some of the lowest values were observed in the Czech Republic (CZE1_2) and Austria (AUT2_2). While high HIX values (> 10) have been linked to the presence of complex molecules and strongly humified organic material, mainly of terrestrial origin, low values (<4) have been associated with autochthonous OM (Huguet et al., 2009). The fluorescence index (FI) covered almost the full range of this index, from a value of 1.3, representing terrestrial sources (degraded plant and soil OM; lower values), in GBR1_2, to a value of 1.8, indicating microbial sources (including extracellular release and leachate from bacteria and algae) in ESP2_2, ESP3_3 (Cory et al., 2007; McKnight et al., 2001). The freshness index, typically associated with the contribution of

recently produced microbial-derived DOM (Parlanti et al., 2000), also spanned a wide range from 0.34 to 0.91 and was positively correlated to the FI and negatively correlated to the HIX and $SUVA_{254}$ (Fig. 4).

The wide distribution of DOM composition between sites indicated differences in the source, processing pathways and biological reactivity of the DOM, as shown by the PCA analysis (Fig. 5). The first principal component (PC1) explained 41% of the total variance across 21 European sites (Fig. 5a). Positive loadings on PC1 were associated with high TOC, A_{254} and HIX, indicating a terrestrial DOM signature. In contrast, negative loadings of PC1 were found for agricultural land use, NO_3^-, SO_4^{2-}, Ca^{2+}, fluorescence Peak T and Peak M, freshness index and FI, likely associated with fresh and recently produced algal and microbial DOM (Ohno, 2002). Running waters from Great Britain (GBR1_1; GBR1_2), Sweden (SWE1_1, SWE2_1) and Austria (AUT1_1, AUT1_2) were characterized by low anions, cations and high concentrations of terrestrial humidified DOM (positive scores in PC1 Fig. 5b). In contrast, negative scores (Fig. 5b) of running waters from Spain (ESP) and the Czech Republic indicated an enrichment in nutrients and fresh autochthonous OM. Also, negative loadings for the percentage of urban and agricultural areas in the studied catchments suggest that anthropogenic activities might enrich running waters in nutrients and enhance primary production (Fig. 5a). The second component (PC2) explained 14% of the variance. Positive loadings on PC2 were found for the fluorescence Peak A and the ratio of the Peaks A to C (A/C). Both Peaks A and C have been linked to the presence of humic substances (Fellman et al., 2010). However, an increase in the relative abundance of the peak A compared to Peak C (A/C peak ratio) has been related to DOM processing, as Peak C is lost preferentially to Peak A under both photo- and biodegradation processes (Kothawala et al., 2012). Therefore, positive loadings of PC2 indicated terrestrial DOM that had been processed (Fig. 5a). On the opposite end, negative loadings on PC2 were associated with aromatic compounds ($SUVA_{254}$) (Weishaar et al., 2003) and terrestrial DOM (Peak C) yet not strongly degraded (Kothawala et al., 2012).

3.4 Predictors of THg, MeHg and %MeHg Concentrations

A PLS model (PLS model I, Fig. 6) identified key factors driving THg_T concentrations in running waters. From the 29 available sites, only 21 sites were included in the PLS model which contained a complete set of required variables. To interpret the PLS loading plots, the distance and positioning of Y variables (THg, MeHg or %MeHg) relative to X variables indicated how well, or poorly, they related to each other. The greater the distance a variable (X or Y) lies from the origin, the greater its overall influence. Variables situated close together on the PLS plot are positively correlated, while variables opposite to each other are negatively correlated. The proportion of variance in the X variables (i.e. DOM composition, anions, cations and environmental factors) explained by the model is indicated by the R^2X. The R^2Y value indicates the proportion of variance in THg explained by the model. With two predictive components (R^2X, 50%), the variance of THg concentrations was well explained (R^2Y, 83.2%) and relatively well predicted (Q^2, 60%) by the PLS model I (Fig. 6, Table S5, Table S6). PLS model I indicates that while TOC and A_{254} presented the highest positive correlation with THg, freshness index, FI and agriculture were negatively correlated. When not including sites highly influenced by terrestrial DOM inputs, GBR1_1 and GBR1_2, a second PLS (PLS model II), with two predictive components (R^2X, 40%), explained the variance of THg_T concentrations relatively well (R^2Y, 82%) but could not predict them (Q^2, -2%) (Table S7).

It was not possible to predict a significant proportion of the variability in MeHg concentrations using a PLS model with the measured variables. Nevertheless, the concentration of MeHg was significantly correlated to %MeHg (Fig. 4). Additionally, the %MeHg was significantly and positively correlated to Peak M (%), FI and sulfate concentration and negatively related to HIX and THg_T (Fig. 4).

4. Discussion

4.1 Hg levels in European running waters

Our results provide new information on THg and MeHg concentrations in streams at a European scale. THg concentrations across the studied European running waters were in the

same range as those measured in pristine streams of northern Sweden (Eklöf et al., 2012), USA (Oregon, Wisconsin and Florida, Brigham et al., (2009); California, Tsui et al., (2009) and Minnesota, Balogh et al., (2002)) and France (Cavalheiro et al., 2016) and were lower than those reported for rivers typically contaminated by point sources (Baptista-Salazar et al., 2017; Bravo et al., 2014). Therefore, none of the study sites appeared to be affected by point sources of Hg.

Fluvial systems are an important transport pathway and ultimately deliver Hg originating from catchment soils to the marine environment. At a broader scale, we attempted to provide a rough estimate discharge of THg_T and $MeHg_T$ of European rivers considering median values obtained in this study and the total European river discharge (3100 km^3) (Shiklomanov and Rodda, 2004). Without considering point source of contamination, such as chlor-alkali or mining activities, known to increase stream Hg concentrations, the estimated European river discharge of THg_T and $MeHg_T$ would be 1426 kg $year^{-1}$ (IQR: 868 – 2494) and 97 kg $year^{-1}$ (IQR: 60 – 254), respectively. Particles are an important vector of Hg transport in streams (Schuster et al., 2011) and can influence hydrologically mediated processes such as sedimentation and/or remobilization (e.g heavy rain events) of Hg previously deposited within river systems, which can largely affect THg_T and $MeHg_T$ loads (Baptista-Salazar et al., 2017; Moreno-Brush et al., 2016; Sunderland and Mason, 2007). Measured THg and MeHg concentrations were notably higher in the total fraction compared to the dissolved fraction, highlighting the role of particles in the transport and fate of Hg in the studied fluvial systems. As precise hydrological data were unavailable here, and our calculations are based on a single sampling campaign, and the discharge of THg and MeHg only provides an initial rough estimate to be considered with care. In order to improve upon current estimates of European Hg discharge into the oceans (Kocman et al., 2017), greater monitoring of THg and MeHg is required across fluvial systems, particularly beyond the boreal ecozone.

4.2 Terrestrial DOM: An Important Source of THg in European Running Waters

444 Using a multivariate approach comparing 21 streams spanning a wide geographical
445 area across Europe, we were able to discriminate between the relative influence of bulk
446 DOM optical characteristics and environmental variables on THg and MeHg concentrations.
447 PC1 of the PLS model showed positive correlations between the highly influential predictors
448 TOC and A_{254} with THg concentrations in the studied sites and suggests that terrestrial DOM
449 is an important driver of THg in streams (Fig. 6). Sites characterized by humic-rich soils, such
450 as those in Sweden and Great Britain (Jones et al., 2005), presented the highest THg_T and
451 THg_D concentrations. The positive correlation between terrestrial DOM and THg
452 concentration in boreal rivers and streams has been previously reported in the literature
453 (Brigham et al., 2009; Eklöf et al., 2012). As atmospheric Hg deposition during the industrial
454 era have led to the accumulation of Hg in organic rich soils (Johansson and Tyler, 2001), the
455 remobilization of Hg-enriched soil OM is an important process controlling THg concentrations
456 in streams (Baptista-Salazar et al., 2017; Brigham et al., 2009; Driscoll et al., 1995; Eklöf et
457 al., 2012; Kirk and Louis, 2009; Tsui et al., 2009) and lakes (Bravo et al., 2017).
458 It is noteworthy to highlight the lack of a significant correlation between TOC and
459 THg_T concentration ($p = 0.6$) when the sites with the highest TOC and THg_T concentrations
460 (SWE2_1, GBR1_1 and GBR1_2) were excluded from the statistical analyses. Also, a poor
461 predictability was obtained in a PLS model (PLS model II) built for THg_T excluding the sites
462 highly influenced by terrestrial DOM (GBR1_1 and GBR1_2, Table S7). Therefore, TOC, and
463 DOM components associated with terrestrial DOM, failed to predict THg_T concentrations in
464 southern parts of Europe (FRA, ESP, CZE, AUT, BGR and DEU). This suggests that other
465 Hg sources are relevant for the studied southern streams. Direct inputs of Hg deposited by
466 wet and dry atmospheric depositional processes (Brigham et al., 2009; Domagalski et al.,
467 2016; Lee et al., 2001) could contribute to THg_T concentrations in streams with low inputs of
468 terrestrial DOM. Besides atmospheric deposition, catchment characteristics and changes in
469 runoff may be relevant in determining THg_T in streams and rivers (Baptista-Salazar et al.,
470 2017; Domagalski et al., 2016). Therefore, our results confirm the role of terrestrial OM as an
471 important source of Hg for streams but highlight the uncertainties on the drivers of THg

concentrations at broader global scale when considering systems with low loads of terrestrial OM.

4.3 Autochthonous DOM and Nutrients: Important Drivers of MeHg Formation in European Running Waters

In this study, MeHg concentrations measured in running waters were in the same range as those previously reported for Sweden (Skyllberg et al., 2003), USA (California, Tsui et al., (2009); Florida, Brigham et al., (2009)) and France (Cavalheiro et al., 2016). Similarly, the %MeHg measured in samples collected in Sweden and Great Britain were similar to those previously reported in the literature (Brigham et al., 2009; Skyllberg et al., 2003). In contrast to THg, MeHg concentrations were not correlated to TOC, A_{254} or HIX (Fig. 4), suggesting that terrestrial sources are not the main vector for MeHg in the studied streams. MeHg concentrations have been related to the concentration of autochthonous OM in reservoirs, lakes and in the Baltic sea (Gascon Diez et al., 2016; Noh et al., 2017; Soerensen et al., 2017).

The %MeHg has been considered a proxy of net MeHg formation (Drott et al., 2008). In the studied European streams studied here, the positive correlation between %MeHg to Peak M and the FI indicated that autochthonous OM is important for MeHg formation. Peak M, as well as Peak A and Peak C, have been generally described as humic-like peaks (Fellman et al., 2010). Peaks A and C have been linked to DOM derived primarily from vascular plant sources, aromatic and with a higher-molecular-weight fraction of the DOM pool (Coble, 1996). In contrast, Peak M represents compounds less aromatic and of lower molecular weight as compared to peaks A and C (Fellman et al., 2010). In a previous study performed in freshwaters, strong correlations between Peak M and Peak T (protein-like) were reported, but weaker relationships were observed between Peak M and Peaks A and C (Kothawala et al., 2014). Indeed, Peak M was originally used as a marker for autochthonous DOM from planktonic production (Fellman et al., 2010). A positive correlation of the %MeHg with Peak M and the FI thus suggests that net MeHg production is linked to fresh autochthonous OM. In contrast, the negative correlation between %MeHg and HIX suggests

that high concentrations of highly humified terrestrial DOM hampered Hg methylation processes most likely by decreasing Hg bioavailability (Chiasson-Gould et al., 2014; Soerensen et al., 2017) and/or bacterial activity (Bravo et al., 2017). High Hg methylation rates have been associated with algal derived OM (Bravo et al., 2017; Gascon Diez et al., 2016; Herrero Ortega et al., 2018; Mazrui et al., 2016). Our study provides further evidence of the potential role of algal and/or microbial DOM in the *in situ* formation of MeHg in streams.

The methylation of IHg to MeHg in aquatic systems has been primarily attributed to the activity of sulfate-reducing bacteria, iron-reducing bacteria (FeRB), methanogens and Firmicutes (Gilmour et al., 2013) in oxygen limiting conditions of sediments (Bravo et al., 2017), hypolimnion (Eckley and Hintelmann, 2006) and settling particles (Gascon Diez et al., 2016). As sulfate can be used as an electron acceptor by Hg methylating microorganisms (Pak and Bartha, 1998), the positive significant correlation found between the %MeHg and the sulfate concentration, suggests an important role of SRB in MeHg formation in running waters and provides further evidence for the relevance of *in situ* MeHg formation.

Stream sulfate mainly originates from atmospheric deposition and/or geogenic sources (Ledesma et al., 2018). Because sulfate release is accompanied by cation leaching (Prechtel et al., 2001), high concentrations of both sulfate and cations (e.g. calcium, Table S2) in Spanish sites indicate an effect of geological substrate of the river basin on the stream water chemistry. Although it was not the focus of this work, these results underline the relevance of geology and catchment characteristics on stream water properties and ultimately also for Hg cycling.

Conclusion

Our findings indicated that streams enriched in terrestrial DOM, as typical of Northern study sites, revealed the highest THg concentrations, suggesting the source was from organic rich catchment soils. In contrast, Southern European streams were enriched in nutrients and autochthonous DOM and although inputs of THg and terrestrial DOM from the

catchment were lower, we propose that MeHg levels were regulated by. We propose that the elevated MeHg concentrations in some of these sites could be due to a higher *in situ* MeHg formation, likely related to enhanced microbial activity, which is boosted by the availability of autochthonous algal/microbial derived DOM and sulfate. Our results show the interplay between DOM components and THg and MeHg concentrations in streams and provide new insights into Hg cycling in aquatic systems at a broad geographical European scale.

References

Amos, H.M., Jacob, D.J., Kocman, D., Horowitz, H.M., Zhang, Y., Dutkiewicz, S., Horvat, M., Corbitt, E.S., Krabbenhoft, D.P., Sunderland, E.M., 2014. Global biogeochemical implications of mercury discharges from rivers and sediment burial. Environ. Sci. Technol. 48, 9514–9522. doi:10.1021/es502134t

Amos, H.M., Jacob, D.J., Streets, D.G., Sunderland, E.M., 2013. Legacy impacts of all-time anthropogenic emissions on the global mercury cycle. Global Biogeochem. Cycles 27, 410–421. doi:10.1002/gbc.20040

Balogh, S.J., Huang, Y., Offerman, H.J., Meyer, M.L., Johnson, D.K., 2002. Episodes of elevated methylmercury concentrations in prairie streams. Environ. Sci. Technol. 36, 1665–1670. doi:10.1021/es011265w

Baptista-Salazar, C., Richard, J.H., Horf, M., Rejc, M., Gosar, M., Biester, H., 2017. Grain-size dependence of mercury speciation in river suspended matter, sediments and soils in a mercury mining area at varying hydrological conditions. Appl. Geochemistry 81, 132–142. doi:10.1016/j.apgeochem.2017.04.006

Bravo, A.G., Bouchet, S., Guédron, S., Amouroux, D., Dominik, J., Zopfi, J., 2015. High methylmercury production under ferruginous conditions in sediments impacted by sewage treatment plant discharges. Water Res. 80, 245–255. doi:10.1016/j.watres.2015.04.039

Bravo, A.G., Bouchet, S., Tolu, J., Björn, E., Mateos-Rivera, A., Bertilsson, S., 2017. Molecular composition of organic matter controls methylmercury formation in boreal lakes. Nat. Commun. 8, 14255. doi:10.1038/ncomms14255

Bravo, A.G., Cosio, C., Amouroux, D., Zopfi, J., Chevalley, P.-A., Spangenberg, J.E., Ungureanu, V.-G., Dominik, J., 2014. Extremely elevated methyl mercury levels in water, sediment and organisms in a Romanian reservoir affected by release of mercury from a chlor-alkali plant. Water Res. 49, 391–405.

Brigham, M.E., Wentz, D. a., Aiken, G.R., Krabbenhoft, D.P., 2009. Mercury cycling in stream ecosystems. 1. Water column chemistry and transport. Environ. Sci. Technol. 43, 2720–2725. doi:10.1021/es802694n

Cavalheiro, J., Sola, C., Baldanza, J., Tessier, E., Lestremau, F., Botta, F., Preud'homme, H., Monperrus, M., Amouroux, D., 2016. Assessment of background concentrations of organometallic compounds (methylmercury, ethyllead and butyl- and phenyltin) in French aquatic environments. Water Res. 94, 32–41. doi:10.1016/j.watres.2016.02.010

Chiasson-Gould, S.A., Blais, J.M., Poulain, A.J., 2014. Dissolved organic matter kinetically controls mercury bioavailability to bacteria. Environ. Sci. Technol. 48, 3153–3161. doi:10.1021/es4038484

Chowdhury, S., 2013. Trihalomethanes in drinking water: Effect of natural organic matter distribution. Water 39, 1–8.

Coble, P.G., 1996. Characterization of marine and terrestrial DOM in seawater using excitation-emission matrix spectroscopy. Mar. Chem. 51, 325–346. doi:10.1016/0304-4203(95)00062-3

Cory, R.M., McKnight, D.M., Chin, Y.P., Miller, P., Jaros, C.L., 2007. Chemical characteristics of fulvic acids from Arctic surface waters: Microbial contributions and photochemical transformations. J. Geophys. Res. Biogeosciences 112, 1–14. doi:10.1029/2006JG000343

Dennis, I.F., Clair, T.A., Driscoll, C.T., Kamman, N., Chalmers, A., Shanley, J., Norton, S.A., Kahl, S., 2005. Distribution patterns of mercury in Lakes and Rivers of northeastern North America. Ecotoxicology 14, 113–123. doi:10.1007/s10646-004-6263-0

Domagalski, J., Majewski, M.S., Alpers, C.N., Eckley, C.S., Eagles-Smith, C.A., Schenk, L., Wherry, S., 2016. Comparison of mercury mass loading in streams to atmospheric deposition in watersheds of Western North America: Evidence for non-atmospheric mercury sources. Sci. Total Environ. 568, 638–650. doi:10.1016/j.scitotenv.2016.02.112

584 Driscoll, C.T., Blette, V., Yan, C., Schofield, C.L., Munson, R., Holsapple, J., 1995. The role of
585 dissolved organic carbon in the chemistry and bioavailability of mercury in remote Adirondack
586 lakes. Water, Air, Soil Pollut. 80, 499–508. doi:10.1007/BF01189700

587 Driscoll, C.T., Han, Y.-J., Chen, C.Y., Evers, D.C., Lambert, K.F., Holsen, T.M., Kamman, N.C.,
588 Munson, R.K., 2007. Mercury contamination in forest and freshwater ecosystems in the
589 northeastern United States. Bioscience 57, 17. doi:10.1641/B570106

590 Drott, A., Lambertsson, L., Björn, E., Skyllberg, U., 2008. Do potential methylation rates reflect
591 accumulated methyl mercury in contaminated sediments? Environ. Sci. Technol. 42, 153–158.

592 Eckley, C.S., Hintelmann, H., 2006. Determination of mercury methylation potentials in the water
593 column of lakes across Canada. Sci. Total Environ. 368, 111–125.
594 doi:10.1016/j.scitotenv.2005.09.042

595 Eklöf, K., Fölster, J., Sonesten, L., Bishop, K., 2012. Spatial and temporal variation of THg
596 concentrations in run-off water from 19 boreal catchments, 2000-2010. Environ. Pollut. 164, 102–
597 109. doi:10.1016/j.envpol.2012.01.024

598 Eklöf, K., Kraus, A., Futter, M., Schelker, J., Meili, M., Boyer, E.W., Bishop, K., 2015. Parsimonious
599 model for simulating total mercury and methylmercury in boreal streams based on riparian flow
600 paths and seasonality. Environ. Sci. Technol. 49, 7851–7859. doi:10.1021/acs.est.5b00852

601 Eriksson, L., Johansson, E., Wold, S., 1999. Introduction to Multi- and Megavariate Data Analysis
602 Using Projection Methods (PCA & PLS). Umetrics.

603 Fellman, J.B., Hood, E., Spencer, R.G.M., 2010. Fluorescence spectroscopy opens new windows into
604 dissolved organic matter dynamics in freshwater ecosystems: A review. Limnol. Oceanogr. 55,
605 2452–2462. doi:10.4319/lo.2010.55.6.2452

606 Fitzgerald, W.F., Engstrom, D.R., Mason, R.P., Nater, E.A., 1998. The case for atmospheric mercury
607 contamination in remote Areas. Environ. Sci. Technol. 32, 1–7.

608 Gascon Diez, E., Loizeau, J.-L., Cosio, C., Bouchet, S., Adatte, T., Amouroux, D., Bravo, A.G., 2016.
609 Role of settling particles on mercury methylation in the oxic water column of freshwater systems.
610 Environ. Sci. Technol. 50, 11672–11679. doi:10.1021/acs.est.6b03260

611 Gilmour, C.C., Podar, M., Bullock, A.L., Graham, A.M., Brown, S.D., Somenahally, A.C., Johs, A.,

612 Hurt, R.A., Bailey, K.L., Elias, D.A., 2013. Mercury methylation by novel microorganisms from
613 new environments. Environ. Sci. Technol. 47, 11810–11820. doi:10.1021/es403075t

614 Graham, A.M., Aiken, G.R., Gilmour, C.C., 2013. Effect of dissolved organic matter source and
615 character on microbial Hg methylation in Hg-S-DOM solutions. Environ. Sci. Technol. 47, 5746–
616 5754. doi:10.1021/es400414a

617 Grigal, D.F., 2002. Inputs and outputs of mercury from terrestrial watersheds: a review. Environ. Rev.
618 10, 1–39. doi:10.1139/a01-013

619 Herrero Ortega, S., Catalán, N., Björn, E., Gröntoft, H., Hilmarsson, T.G., Bertilsson, S., Wu, P.,
620 Bishop, K., Levanoni, O., Bravo, A.G., 2018. High methylmercury formation in ponds fueled by
621 fresh humic and algal derived organic matter. Limnol. Oceanogr. 63, S44–S53.
622 doi:10.1002/lno.10722

623 Huguet, A., Vacher, L., Relexans, S., Saubusse, S., Froidefond, J.M., Parlanti, E., 2009. Properties of
624 fluorescent dissolved organic matter in the Gironde Estuary. Org. Geochem. 40, 706–719.
625 doi:10.1016/j.orggeochem.2009.03.002

626 Johansson, K., Tyler, G., 2001. Impact of atmospheric long range transport of lead, mercury and
627 cadmium on the Swedish forest environment. Water, Air Soil Pollut. Focus 1, 279–297.

628 Jones, R.J.A., Hiederer, R., Rusco, E., Montanarella, L., 2005. Estimating organic carbon in the soils
629 of Europe for policy support. Eur. J. Soil Sci. 56, 655–671. doi:10.1111/j.1365-
630 2389.2005.00728.x

631 Jonsson, S., Skyllberg, U., Nilsson, M.B., Lundberg, E., Andersson, A., Björn, E., 2014. Differentiated
632 availability of geochemical mercury pools controls methylmercury levels in estuarine sediment
633 and biota. Nat. Commun. 5, 4624. doi:10.1038/ncomms5624

634 Kirk, J.L., Louis, V.L.S., 2009. Multiyear total and methyl mercury exports from two major sub-arctic
635 rivers draining into Hudson Bay, Canada. Environ. Sci. Technol. 43, 2254–2261.
636 doi:10.1021/es803138z

637 Kocman, D., Wilson, S.J., Amos, H.M., Telmer, K.H., Steenhuisen, F., Sunderland, E.M., Mason, R.P.,
638 Outridge, P., Horvat, M., 2017. Toward an assessment of the global inventory of present-day
639 mercury releases to freshwater environments. Int. J. Environ. Res. Public Health 14.

640 doi:10.3390/ijerph14020138

641 Kothawala, D., Stedmon, C., Müler, R., Weyhenmeyer, G., Köhler, S., Tranvik, L.J., 2014. Controls of
642 dissolved organic matter quality : evidence from a large-scale boreal lake survey. Glob. Chang.
643 Biol. 20, 1101–1114. doi:10.1111/gcb.12488

644 Kothawala, D.N., von Wachenfeldt, E., Koehler, B., Tranvik, L.J., 2012. Selective loss and
645 preservation of lake water dissolved organic matter fluorescence during long-term dark
646 incubations. Sci. Total Environ. 433, 238–246. doi:10.1016/j.scitotenv.2012.06.029

647 Ledesma, J.L.J., Futter, M.N., Blackburn, M., Lidman, F., Grabs, T., Sponseller, R.A., Laudon, H.,
648 Bishop, K.H., Köhler, S.J., 2018. Towards an Improved Conceptualization of Riparian Zones in
649 Boreal Forest Headwaters. Ecosystems 21, 297–315. doi:10.1007/s10021-017-0149-5

650 Lee, D.S., Nemitz, E., Fowler, D., Kingdon, R.D., 2001. Modelling atmospheric mercury transport and
651 deposition across Europe and the UK 35, 5455–5466.

652 Lescord, G.L., Emilson, E.J.S., Johnston, T.A., Branfireun, B.A., Gunn, J.M., 2018. Optical Properties
653 of Dissolved Organic Matter and Their Relation to Mercury Concentrations in Water and Biota
654 Across a Remote Freshwater Drainage Basin. Environ. Sci. Technol. acs.est.7b05348.
655 doi:10.1021/acs.est.7b05348

656 Marvin-DiPasquale, M., Lutz, M.A., Brigham, M.E., Krabbenhoft, P., Aiken, G.R., Orem, W.H., Hall,
657 B.D., Lutz, M.A., Brigham, M.E., Krabbenhoft, D.P., 2009. Production and Bed Sediment. 2. Pore
658 Water Partitioning Mercury Cycling in Stream Methylmercury Production and Bed Sediment -
659 Pore Water Partitioning. Environ. Sci. Technol. 43, 2726–2732. doi:10.1021/es802698v

660 Mason, R.P., Choi, A.L., Fitzgerald, W.F., Hammerschmidt, C.R., Lamborg, C.H., Soerensen, A.L.,
661 Sunderland, E.M., 2012. Mercury biogeochemical cycling in the ocean and policy implications.
662 Environ. Res. 119, 101–117. doi:10.1016/j.envres.2012.03.013

663 Mazrui, N.M., Jonsson, S., Thota, S., Zhao, J., Mason, R.P., 2016. Enhanced availability of mercury
664 bound to dissolved organic matter for methylation in marine sediments. Geochim. Cosmochim.
665 Acta 194, 153–162. doi:10.1016/j.gca.2016.08.019

666 McKnight, D.M., Boyer, E.W., Westerhoff, P.K., Doran, P.T., Kulbe, T., Andersen, D.T., 2001.
667 Spectrofluorometric characterization of dissolved organic matter for indication of precursor

668 organic material and aromaticity. Limnol. Oceanogr. 46, 38–48. doi:10.4319/lo.2001.46.1.0038

669 Mevik, B.-H., Wehrens, R., 2007. The pls Package: Principal Component and Partial Least Squares
670 Regression in R. J. Stat. Software, Artic. 18.

671 Monperrus, M., Krupp, E., Amouroux, D., Donard, O.F.., Rodríguez Martín-Doimeadios, R.., 2004.
672 Potential and limits of speciated isotope-dilution analysis for metrology and assessing
673 environmental reactivity. TrAC Trends Anal. Chem. 23, 261–272. doi:10.1016/S0165-
674 9936(04)00313-9

675 Morel, F.M.M., Kraepiel, A.M.L., Amyot, M., 1998. The chemical cycle and bioaccumulation of
676 mercury. Annu. Rev. Ecol. Syst. 29, 543–566. doi:10.1146/annurev.ecolsys.29.1.543

677 Moreno-Brush, M., Rydberg, J., Gamboa, N., Storch, I., Biester, H., 2016. Is mercury from small-scale
678 gold mining prevalent in the southeastern Peruvian Amazon? Environ. Pollut. 218, 150–159.
679 doi:10.1016/j.envpol.2016.08.038

680 Noh, S., Kim, J., Hur, J., Hong, Y., Han, S., 2017. Potential contributions of dissolved organic matter to
681 monomethylmercury distributions in temperate reservoirs as revealed by fluorescence
682 spectroscopy. Environ. Sci. Pollut. Res. doi:10.1007/s11356-017-0913-2

683 Ohno, T., 2002. Fluorescence inner-filtering correction for determining the humification index of
684 dissolved organic matter. Environ. Sci. Technol. 36, 742–746. doi:10.1021/es0155276

685 Pak, K., Bartha, R., 1998. Mercury methylation and demethylation in anoxic lake sediments and by
686 strictly anaerobic bacteria. Appl. Environ. Microbiol. 64, 1013–1017.

687 Parlanti, E., Wörz, K., Geoffroy, L., Lamotte, M., 2000. Dissolved organic matter fluorescence
688 spectroscopy as a tool to estimate biological activity in a coastal zone submitted to
689 anthropogenic inputs. Org. Geochem. 31, 1765–1781. doi:10.1016/S0146-6380(00)00124-8

690 Prechtel, A., Alewell, C., Armbruster, M., Bittersohl, J., Cullen, J.M., Evans, C.D., Helliwell, R.,
691 Kopácek, J., Marchetto, A., Matzner, E., Meesenburg, H., Moldan, F., Moritz, K., Veselý, J.,
692 Wright, R.F., 2001. Response of sulphur dynamics in European catchments to decreasing
693 sulphate deposition. Hydrol. Earth Syst. Sci. 5, 311–326. doi:10.5194/hess-5-311-2001

694 R Core Team, 2016. R: A Language and Environment for Statistical Computing.

695 Rodriguez Martín-Doimeadios, R.C., Monperrus, M., Krupp, E., Amouroux, D., Donard, O.F.X., 2003.
696 Using speciated isotope dilution with GC-inductively coupled plasma MS to determine and
697 unravel the artificial formation of monomethylmercury in certified reference sediments. Anal.
698 Chem. 75, 3202–3211. doi:10.1021/ac026411a

699 Schaefer, J.K., Kronberg, R.-M., Morel, F.M.M., Skyllberg, U., 2014. Detection of a key Hg methylation
700 gene, *hgcA*, in wetland soils. Environ. Microbiol. Rep. 6, 441–447. doi:10.1111/1758-2229.12136

701 Schaefer, J.K., Morel, F.M.M., 2009. High methylation rates of mercury bound to cysteine by
702 *Geobacter sulfurreducens*. Nat. Geosci. 2, 123–126. doi:10.1038/ngeo412

703 Schartup, A.T., Balcom, P.H., Soerensen, A.L., Gosnell, K.J., Calder, R.S.D., Mason, R.P.,
704 Sunderland, E.M., 2015a. Freshwater discharges drive high levels of methylmercury in Arctic
705 marine biota. Proc. Natl. Acad. Sci. 112, 11789–11794. doi:10.1073/pnas.1505541112

706 Schartup, A.T., Mason, R.P., Balcom, P.H., Hollweg, T.A., Chen, C.Y., 2013. Methylmercury
707 production in estuarine sediments: Role of organic matter. Environ. Sci. Technol. 47, 695–700.

708 Schartup, A.T., Ndu, U.C., Balcom, P.H., Mason, R.P., Sunderland, E.M., 2015b. Contrasting effects
709 of marine and terrestrially derived dissolved organic matter on mercury speciation and
710 bioavailability in seawater. Environ. Sci. Technol. 5965–5972.

711 Schuster, P.F., Striegl, R.G., Aiken, G.R., Krabbenhoft, D.P., Dewild, J.F., Butler, K., Kamark, B.,
712 Dornblaser, M., 2011. Mercury Export from the Yukon River Basin and Potential Response to a
713 Changing Climate 9262–9267.

714 Shiklomanov, I.A., Rodda, J.C., 2004. World Water Resources at the Beginning of the Twenty-First
715 Century, Cambridge University Press (UK).

716 Skyllberg, U., Bloom, P.R., Qian, J., Lin, C.-M., Bleam, W.F., 2006. Complexation of mercury(II) in soil
717 organic matter: EXAFS evidence for linear two-coordination with reduced sulfur groups. Environ.
718 Sci. Technol. 40, 4174–80.

719 Skyllberg, U., Qian, J., Frech, W., Xia, K., Bleam, W.F., 2003. Distribution of mercury, methyl mercury
720 and organic sulphur species in soil, soil solution and stream of a boreal forest catchment.
721 Biogeochemistry 64, 53–76. doi:10.1023/A:1024904502633

722 Soerensen, A.L., Schartup, A.T., Skrobonja, A., Björn, E., 2017. Organic matter drives high interannual

variability in methylmercury concentrations in a subarctic coastal sea. Environ. Pollut. 229, 531–538. doi:10.1016/j.envpol.2017.06.008

Sunderland, E.M., Mason, R.P., 2007. Human impacts on open ocean mercury concentrations. Global Biogeochem. Cycles 21. doi:10.1029/2006GB002876

Tjerngren, I., Karlsson, T., Björn, E., Skyllberg, U., 2012. Potential Hg methylation and MeHg demethylation rates related to the nutrient status of different boreal wetlands. Biogeochemistry 108, 335–350. doi:10.1007/s10533-011-9603-1

Tsui, M.T.K., Finlay, J.C., Nater, E.A., 2009. Mercury bioaccumulation in a stream network. Environ. Sci. Technol. 43, 7016–7022. doi:10.1021/es901525w

Weishaar, J.L., Aiken, G.R., Bergamaschi, B. a, Fram, M.S., Fujii, R., Mopper, K., 2003. Evaluation of specific ultraviolet absorbance as an indicator of the chemical composition and reactivity of dissolved organic carbon. Environ. Sci. Technol. 37, 4702–4708.

WFD, 2008. Directive 2008/105/EC of 16 December 2008 on environmental quality standards in the field of water policy, amending and subsequently repealing Council Directives 82/176/EEC, 83/513/EEC, 84/156/EEC, 84/491/ECC, 86/280/ECC and amending Directive 2000/60/EC, The European Parliament and the Council of the European Union. Official Journal of the European Union. doi:http://eur-lex.europa.eu/legal-content/EN/TXT/?uri=celex:32008L0105

Wiener, J.G., Krabbenhoft, D.P., Heinz, G.H., Scheuhammer, A.M., 2003. Ecotoxicology of mercury, in: Hoffman, D.J., Rattner, B.A., Jr., G.A.B., Jr., J.C. (Eds.), Handbook of Ecotoxicology, Second Edition. Lewis Publishers, Boca Raton, FL, pp. 409–463. doi:10.1201/9781420032505.ch16

Xia, K., Skyllberg, U., Bleam, W.F., Bloom, P.R., Nater, E.A., Helmke, P.A., 1999. X-ray absorption spectroscopic evidence for the complexation of Hg(II) by reduced sulfur in soil humic substances. Env. Sci Technol 33, 257–261.

Zsolnay, A., Baigar, E., Jimenez, M., Steinweg, B., Saccomandi, F., 1999. Differentiating with fluorescence spectroscopy the sources of dissolved organic matter in soils subjected to drying. Chemosphere 38, 45–50. doi:10.1016/S0045-6535(98)00166-0

Acknowledgements

This research was partially funded the Generalitat de Catalunya (Beatriu de Pinos BP-00385-2016) grants to AGB. DNK would like to acknowledge the Swedish National Science Foundation, Vetenskapsrådet (VR), for a starting grant. We thank the initiators of the first Collaborative European Freshwater Science Project for Young Researchers, the European Federation of Freshwater Sciences (EFFS) board, the European Fresh and Young Researchers (EFYR) and the representatives of the Fresh Blood for Fresh Water (FBFW) meetings. We also thank the seven national freshwater societies financing this project, namely the Deutsche Gesellschaft für Limnologie e.V. (DGL; Germany), Swiss Society for Hydrology and Limnology (Switzerland), Iberian Association for Limnology (AIL; Spain and Portugal), Italian Association of Oceanography and Limnology (Italy), Freshwater Biological Association (FBA; United Kingdom), French Limnological Association (AFL; France), Group of Austrian Members of SIL (SIL-Austria), as well as the Leibniz-Institute of Freshwater Ecology and Inland Fisheries for additional funds. CML was funded by the French Agency for Biodiversity (ONEMA-AFB, Action 13, “Colmatage, échange snappe-rivière et processus biogéochimiques). NC held a “Juan de la Cierva” postdoctoral grant (FJCI-2014-23064). Furthermore, we would like to thank Christian Noss, Elvira de Eyto, Brian C. Doyle, Adam Bednařík, Tea Basic, Georgina Busst, David Fletcher, Danny Sheath, Laura Barral-Fraga, Anna Freixa, Xisca Timoner, Marcus Klaus, Wiebke Schulz, Nina Pansch, Nikolay Simov and Lyubomir A. Kenderov for field assistance, Christoffer Bergvall for laboratory assistance and Viktor Rosenberg for the GIS map. David Kocman is acknowledged for the discussion on Hg loads in rivers.

Authors Contribution:

AGB conceived the study. KA and PB coordinated the sampling and the teams involved in the study. AGB and ET performed GC–ICP–MS analyses of Hg with guidance from DA. DNK conducted fluorescence, spectrometry and DOC and TOC analyses. KA measured cations and anions. AGB and DNK conducted all statistical analyses. AGB, DNK and KA built the figures. AGB wrote the manuscript with significant assistance and comments from DNK, DA,

KA and PB. The rest of the co-authors carried out the sampling and contributed to the writing of the MS.

Table 1. Concentrations of inorganic-Hg (IHg), methylmercury (MeHg), total-Hg (THg = IHg+ MeHg) and the percentage of MeHg as THg (%MeHg) in the dissolved (filtered 0.45 µm: $_D$) and total (unfiltered: $_T$) fraction of the studied streams.

Country	Stream ID	IHg_D	$MeHg_D$	THg_D	$MeHg_D$	IHg_T	$MeHg_T$	THg_T	$MeHg_T$
		ng L^{-1}	pg L^{-1}	ng L^{-1}	%	ng L^{-1}	pg L^{-1}	ng L^{-1}	%
Austria	AUT1_1	1.04	12	1.05	1.2	0.96	16	0.97	1.6
	AUT1_2	0.8	19	0.82	2.3	0.93	19	0.95	2.0
	AUT2_1	0.14	38	0.18	21.1	0.52	54	0.57	9.5
	AUT2_2	0.06	7	0.06	10.4	0.05	8	0.06	13.0
	AUT2_3	0.2	9	0.21	4.4	0.34	26	0.37	7.0
Bulgaria	BGR1_1	0.19	24	0.21	11.4	0.26	27	0.28	9.8
	BGR1_2	0.2	39	0.24	16.4	0.23	31	0.26	12.0
Czech Rep	CZE1_1	0.45	53	0.51	10.4	nd	nd	nd	nd
	CZE1_2	0.24	7	0.25	2.8	0.64	112	0.75	15.0
Germany	DEU1_1	0.17	67	0.23	28.7	0.3	12	0.31	3.9
	DEU1_2	0.14	36	0.17	20.8	0.34	60	0.4	15.0
	DEU2_1	0.14	10	0.15	6.7	0.4	56	0.46	12.2
	DEU2_2	0.11	26	0.13	20.1	0.55	52	0.6	8.7
Spain	ESP1_1	0.3	67	0.37	18.2	0.37	89	0.46	19.3
	ESP1_2	0.22	16	0.24	6.7	0.13	14	0.14	9.7
	ESP1_3	0.16	122	0.28	43.0	0.21	159	0.37	43.1
	ESP2_1	0.14	38	0.17	21.8	0.1	31	0.13	23.5
	ESP2_2	0.53	52	0.58	9.1	0.86	76	0.94	8.1
	ESP2_3	0.5	53	0.56	9.6	0.14	65	0.2	32.5
France	FRA1_1	0.47	15	0.48	3.1	0.49	15	0.51	2.9
	FRA1_2	0.39	17	0.41	4.2	0.86	20	0.88	2.2
Great Britain	GBR1_1	2.17	134	2.3	5.8	2.66	124	2.78	4.5
	GBR1_2	nd	nd	nd	nd	2.31	24	2.33	1.0
	GBR2_1	0.19	45	0.24	19.2	0.33	88	0.42	20.9
	GBR2_2	0.14	17	0.16	11.1	0.27	15	0.28	5.4
Portugal	PRT1_1	0.25	20	0.27	7.5	nd	nd	nd	nd
Sweden	SWE1_1	nd	nd	nd	nd	0.44	89	0.53	16.8
	SWE2_1	0.48	135	0.61	21.9	0.7	153	0.86	17.8
	SWE2_2	0.13	26	0.16	16.2	0.15	30	0.18	16.4

Figure 1. Distribution of the 29 sampling sites across nine European countries (see exact coordinates in Table 1).

Figure 2. Box and whisker plots of the distribution of a) total Hg (THg) in the unfiltered (total) fraction THg_T and the filtered (dissolved) fraction THg_D (n = 27), b) inorganic Hg (IHg) in the total IHg_T and dissolved fractions IHg_D (n = 27), c) monomethyl-Hg (MeHg) concentrations (n = 27) in the total ($MeHg_T$) and dissolved ($MeHg_D$) fractions and d) the %MeHg (n = 27). Boxes represent 25^{th} (Q1) and 75^{th} (Q3) percentile. The median is indicated within the box. The lower whiskers represent the lowest value within 1.5 IQR of the Q1, and the highest within 1.5 IQR of Q3.

Figure 3. Excitation-emission matrixes from sites presenting contrasted DOM characteristics a) and b) show samples with an eminently terrestrially derived DOM rich in humic peaks A and C. Plots c) and d) display samples with a marked microbial or algal signature as indicated by the high intensities in the peak T region. Intensities are shown in fluorescence units.

Figure 4. Significant ($p < 0.05$, n=21) correlations between THg_T, $MeHg_T$, the $\%MeHg_T$, DOM optical properties and stream characteristics. The ellipses have their eccentricity parametrically scaled to the Pearson correlation value (narrower ellipses represent higher correlation values). The orientation of the ellipses indicate negative (red) or positive (blue) correlations (scale on the right).

Figure 5. Principal Component Analysis (PCA) of European streams (n = 21) showing the explained variability arising from principle components 1 (PC1) and 2 (PC2) based on bulk optical characteristics of dissolved organic matter (DOM) and environmental variables including stream order and catchment cover, as presented in (a) the loadings plot, and (b) the corresponding scores plot displaying the 21 study sites.

Figure 6. Partial least squares loadings plot predicting the variability of total mercury (THg) concentration (Y variable, red) with several DOM optical properties and geographical and water chemistry characteristics as predictors (X variables). Fluorescence peaks are expressed as percentage of total fluorescence. Variables in blue were identified to be highly influential predictors of THg (with a variable influence on projection of ≥ 1.0)

Graphical Abstract. Conceptual framework of (a) streams characterized by high inputs of terrestrial DOM and high concentrations of THg and (b) streams enriched in microbial/algal DOM depicting high MeHg formation (%MeHg).

Figure 1

Click here to download high resolution image

Figure 2

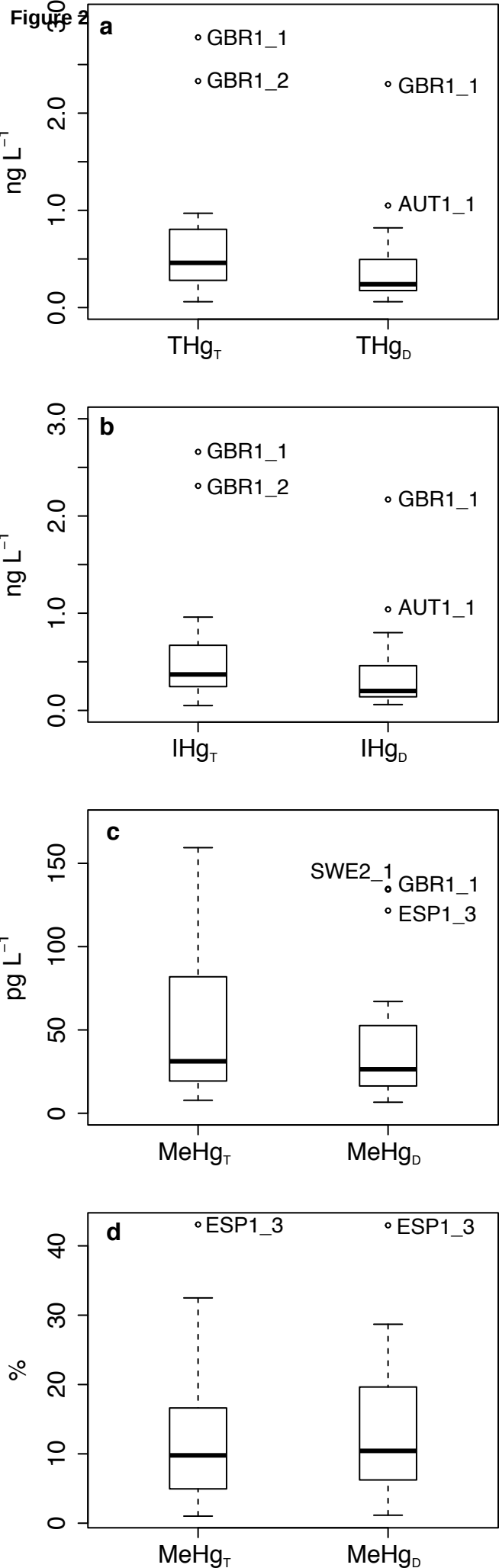
a
GBR1_1
GBR1_2
GBR1_1
AUT1_1
ng L^{-1}
0.0
1.0
2.0
3.0
THg$_T$
THg$_D$
b
GBR1_1
GBR1_2
GBR1_1
AUT1_1
ng L^{-1}
0.0
1.0
2.0
3.0
IHg$_T$
IHg$_D$
c
SWE2_1
GBR1_1
ESP1_3
pg L^{-1}
0
50
100
150
MeHg$_T$
MeHg$_D$
d
ESP1_3
ESP1_3
%
0
10
20
30
40
MeHg$_T$
MeHg$_D$

Figure 3

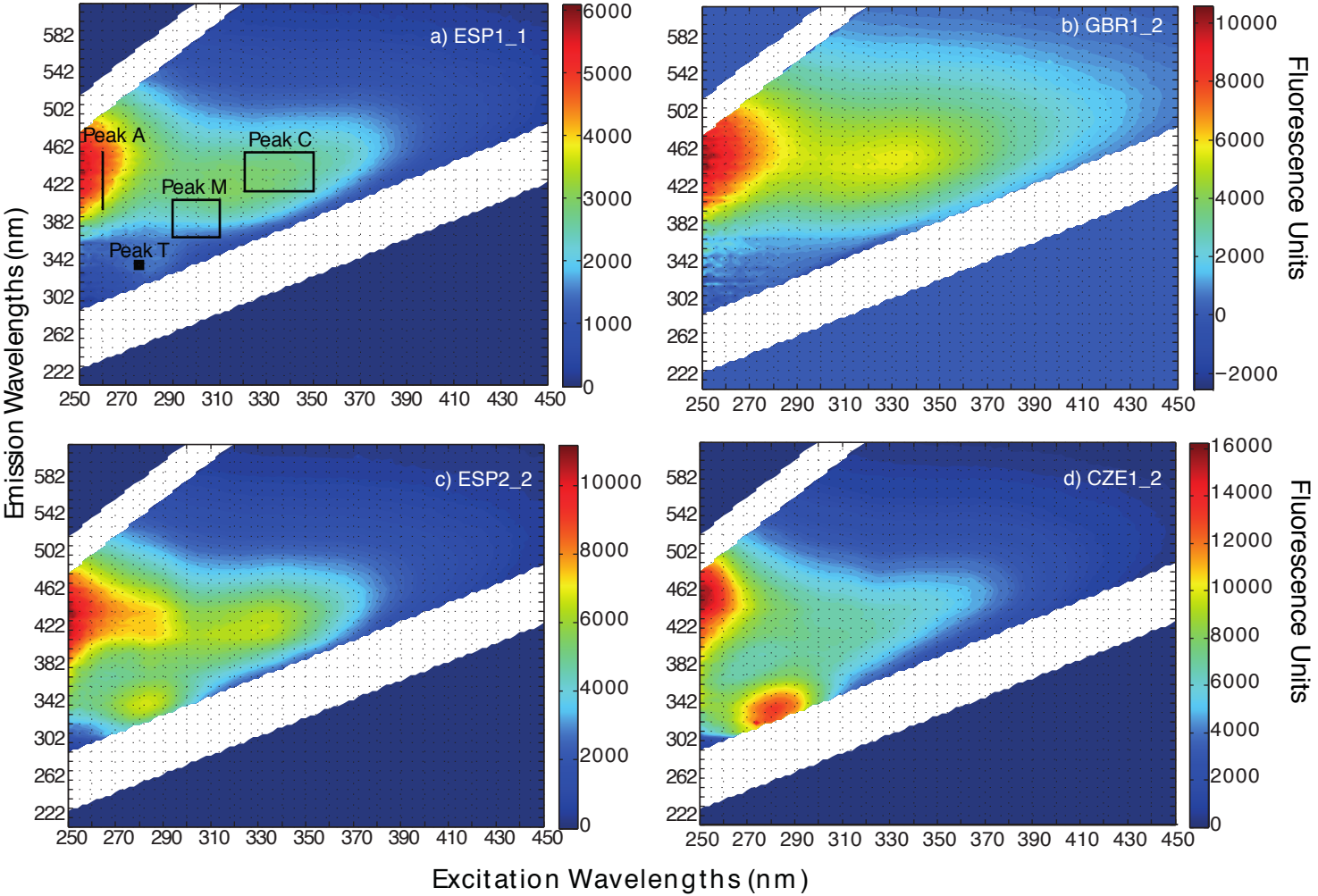
a) ESP1_1
b) GBR1_2
c) ESP2_2
d) CZE1_2
Peak A
Peak C
Peak M
Peak T
Emission Wavelengths (nm)
Excitation Wavelengths (nm)
Fluorescence Units
582
542
502
462
422
382
342
302
262
222
250 270 290 310 330 350 370 390 410 430 450
6000
5000
4000
3000
2000
1000
0
10000
8000
6000
4000
2000
0
−2000
16000
14000
12000
10000
8000
6000
4000
2000
0

Figure 4

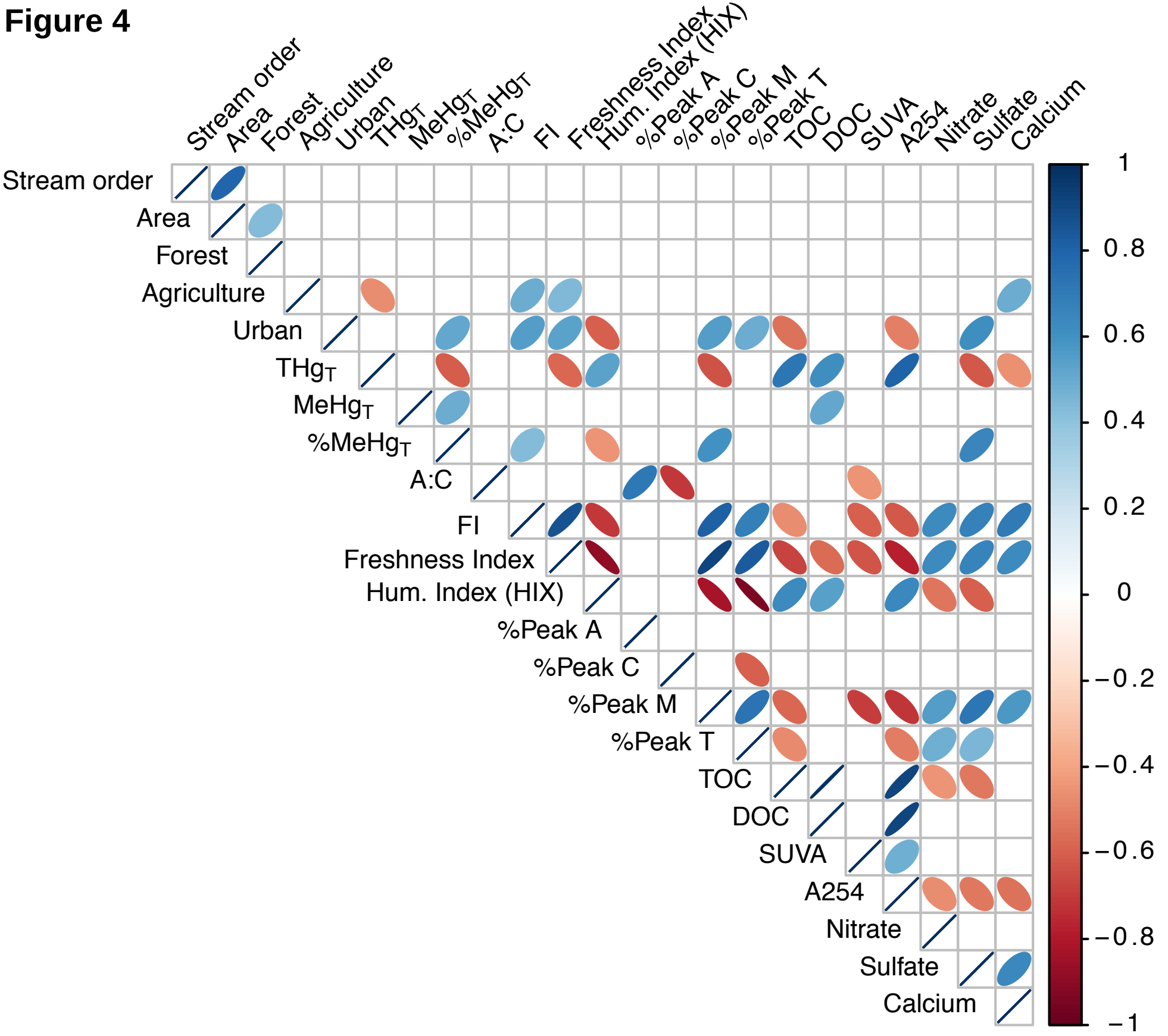
Stream order
Area
Forest
Agriculture
Urban
THgT
MeHgT
%MeHgT
A:C
FI
Freshness Index
Hum. Index (HIX)
%Peak A
%Peak C
%Peak M
%Peak T
TOC
DOC
SUVA
A254
Nitrate
Sulfate
Calcium
1
0.8
0.6
0.4
0.2
0
−0.2
−0.4
−0.6
−0.8
−1

Figure 5

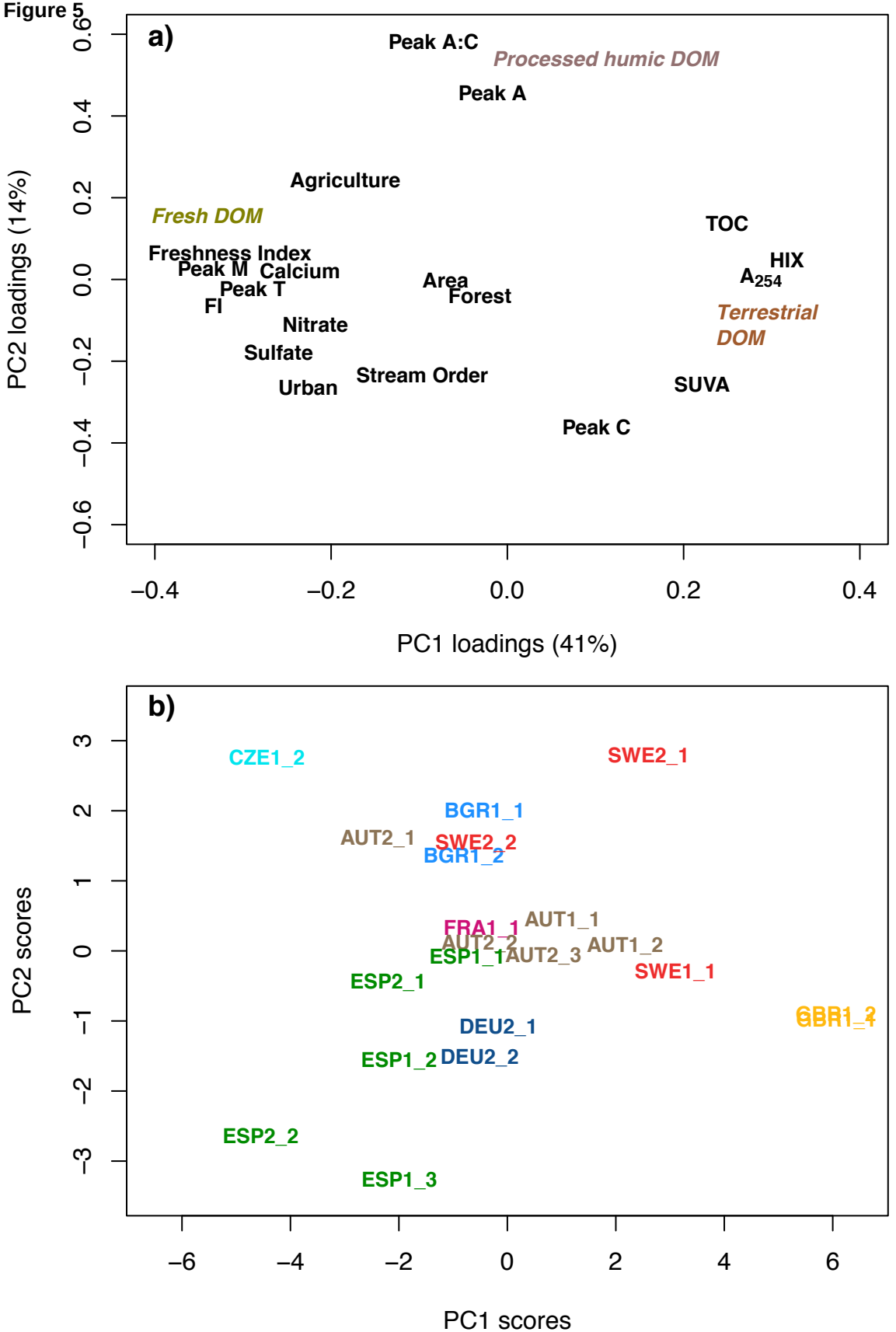
a)
Peak A:C
Processed humic DOM
Peak A
Agriculture
Fresh DOM
TOC
Freshness Index
Peak M
Calcium
Area
HIX
A254
Peak T
Forest
FI
Terrestrial DOM
Nitrate
Sulfate
Stream Order
Urban
SUVA
Peak C
PC2 loadings (14%)
PC1 loadings (41%)
b)
CZE1_2
SWE2_1
BGR1_1
AUT2_1
SWE2_2
BGR1_2
FRA1_1
AUT1_1
AUT2_2
AUT1_2
ESP1_1
AUT2_3
SWE1_1
ESP2_1
GBR1_2
GBR1_1
DEU2_1
ESP1_2
DEU2_2
ESP2_2
ESP1_3
PC2 scores
PC1 scores

Figure 6

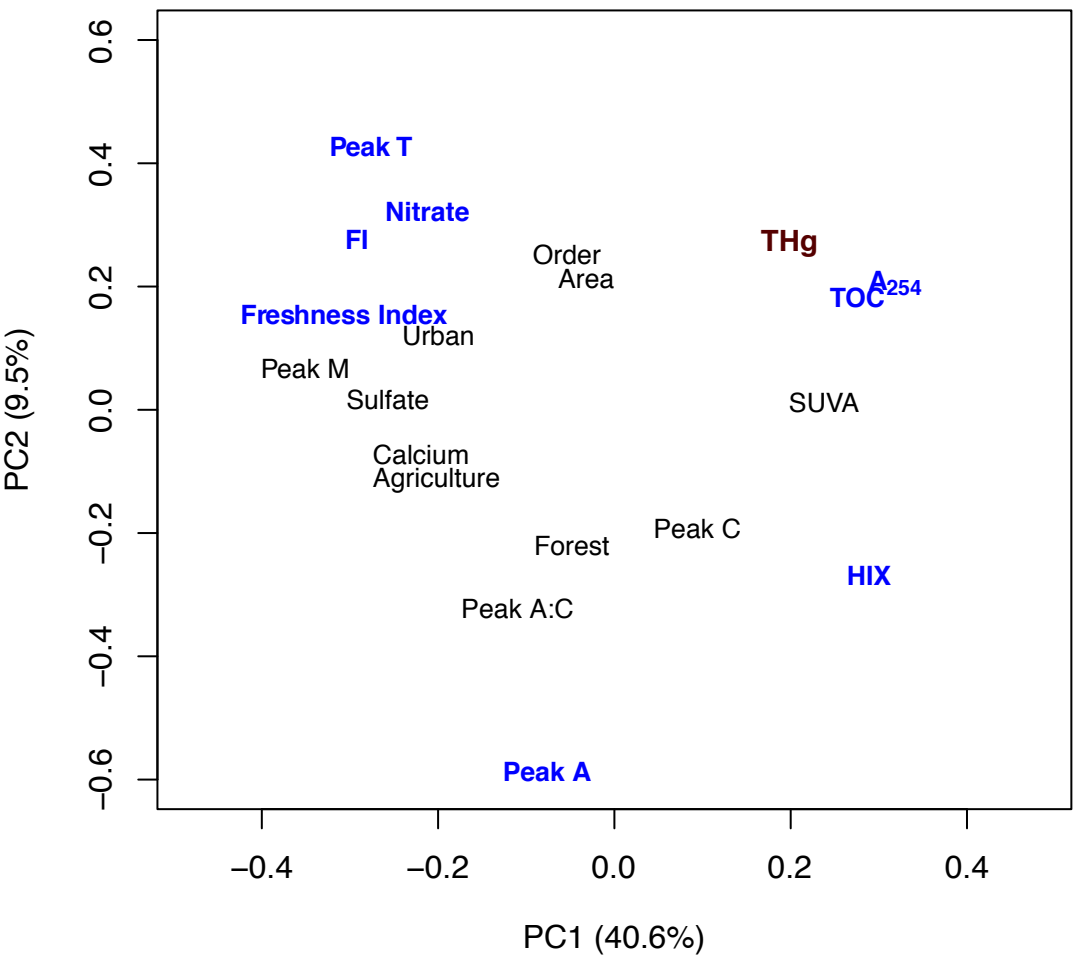
Peak T
Nitrate
FI
Order
Area
THg
A254
TOC
Freshness Index
Urban
Peak M
Sulfate
SUVA
Calcium
Agriculture
Peak C
Forest
HIX
Peak A:C
Peak A
0.6
0.4
0.2
0.0
−0.2
−0.4
−0.6
PC2 (9.5%)
−0.4
−0.2
0.0
0.2
0.4
PC1 (40.6%)

Electronic Supplementary Material (for online publication only)

Click here to download Electronic Supplementary Material (for online publication only): EuroRun_Hg_SI_v4.docx

Method Details (MethodsX)

Click here to download Method Details (MethodsX): MethodsX-Bravo et al_v3.docx.zip